

Crystal Structures and Magnetic Properties of Sparteinium Tetrahalocuprate Monohydrate Compounds

Yong-Min Lee, Sung-Min Park, Sung Kwon Kang,[†] Young-Inn Kim,[‡] and Sung-Nak Choi*

Department of Chemistry and the Chemistry Institute for Functional Materials, Pusan National University, Pusan 609-735, Korea

[†]Department of Chemistry, Chungnam National University, Daejeon 305-764, Korea

[‡]Department of Chemistry Education, Pusan National University, Pusan 609-735, Korea

Received February 20, 2004

The crystal structures of sparteinium tetrachlorocuprate monohydrate $[(C_{15}H_{28}N_2)CuCl_4 \cdot H_2O]$, **1** and sparteinium tetrabromocuprate monohydrate $[(C_{15}H_{28}N_2)CuBr_4 \cdot H_2O]$, **2**, were determined. The structures of **1** [orthorhombic, $P2_12_12_1$, $a = 8.3080(10)$ Å, $b = 14.6797(19)$ Å and $c = 16.4731(17)$ Å], and **2** [orthorhombic, $P2_12_12_1$, $a = 8.4769(7)$ Å, $b = 15.166(3)$ Å and $c = 16.679(3)$ Å], are composed of a doubly protonated sparteinium cation, $[C_{15}H_{28}N_2]^{2+}$, a discrete CuX_4^{2-} anion ($X = Cl^-$ or Br^-), and one water molecule. These monomeric compounds are stabilized through various types of hydrogen bonding interaction in their packing structures. Crystal **2** exhibits weak anti-ferromagnetism ($J = -3.24$ cm⁻¹) as opposed to the magnetically isolated paramagnetism observed for **1**. The results of comparative magneto-structural investigations of **1** and **2** suggest that the pathway for the weak anti-ferromagnetic super-exchange in **2** might be through a $Cu-Br \cdots Br-Cu$ contact.

Key Words : Copper(II), Anti-ferromagnetism, (–)-Sparteine, “Bromide-bromide” contact, Hydrogen bonding

Introduction

The tetrahalometalate compounds with various organic counteranions have been the subject of many theoretical,¹⁻³ structural,⁴⁻⁸ and magneto-structural⁹⁻¹⁶ studies. Among them, the four-coordinate tetrahalocuprate(II) ions have been found to possess a variety of geometries from square-planar to near tetrahedral symmetry and the stereochemistry of the tetrahalocuprate ion is known to be influenced by the nature of the counteranions and by the presence of hydrogen bonding interaction. The magneto-structural relationships in the tetrahalocuprate compounds have been intensively studied, and in view of the weak anti-ferromagnetic interaction in the copper(II)-halide systems, the hydrogen bonding and the “halide-halide” contact (the $Cu-X \cdots X-Cu$ contact) are known to be very important pathways for the magnetic exchange. The magnetic exchange *via* “halide-halide” contact is benefited by the substantial overlap of the magnetic orbitals of the non-bonded halides and is well established for the copper(II)-bromide system.¹⁰⁻¹⁴ The hydrogen bonding in this type of molecule is also known to provide a pathway for the magnetic super-exchange.^{15,16}

In this work, we report on the preparation, crystal structures, and magnetic properties of sparteinium tetrachlorocuprate monohydrate $(C_{15}H_{28}N_2)CuCl_4 \cdot H_2O$, **1** and sparteinium tetrabromocuprate monohydrate $[C_{15}H_{28}N_2]CuBr_4 \cdot H_2O$, **2**, and propose a possible magnetic exchange pathway for the weak anti-ferromagnetic interaction in **2**. (–)-Sparteine base $C_{15}H_{26}N_2$ has been utilized in the preparation of many tetrahedrally distorted copper(II) compounds,¹⁷ and the

choice of this base was determined by the presence of two tertiary amine nitrogen atoms capable of establishing strong hydrogen bonds, which can stabilize the crystal structure of the compounds.

Experimental Section

Materials and Preparation. All reagents and solvents were obtained commercially either from Sigma Chemicals or Aldrich Chemicals. Anhydrous ethanol was distilled from calcium hydride and stored under argon. (–)-Sparteine, $C_{15}H_{26}N_2$ was purchased from Sigma Chemicals and was used without further purification. (–)-Sparteinium tetrachlorocuprate(II) compound was prepared from a direct reaction between $C_{15}H_{26}N_2$ and $CuCl_2 \cdot 2H_2O$. (–)-Sparteine (1.4 mL, 6.09 mmol) dissolved in ethanol (50 mL) was added to an excess of concentrated HCl (15.2 mmol; ~2.5 times of sparteine base). To this solution, 1.03 g (6.04 mmol) of $CuCl_2 \cdot 2H_2O$ dissolved also in ethanol (10 mL) was added. The resulting solution was stirred vigorously for 3 hrs at room temperature and then was refrigerated overnight. The resulting orange-yellow precipitate was filtered off, washed with cold absolute ethanol, and dried in a vacuum. (–)-Sparteinium tetrabromocuprate compound was prepared according to a similar procedure; (–)-sparteine (1.4 mL, 6.09 mmol), dissolved in 50 mL of ethanol-triethylorthoformate mixture (5 : 1 v/v), was added to an excess of concentrated HBr (15.2 mmol; ~2.5 times of sparteine base). To this solution, 1.36 g (6.09 mmol) of anhydrous $CuBr_2$, dissolved in 10 mL of ethanol-triethylorthoformate mixture (5 : 1 v/v), was added. The resulting solution was stirred vigorously for 3 hrs at room temperature and then was refrigerated overnight. The dark violet precipitate which appeared was

*To whom all correspondence should be addressed. Tel: +82-51-510-2238; Fax: +82-51-516-7421; e-mail: sunachoi@pusan.ac.kr

collected by filtration and washed several times with cold ethanol and then, this precipitate was dried under vacuum. Anal. Calcd. for $\text{CuC}_{15}\text{H}_{28}\text{N}_2\text{Cl}_4 \cdot \text{H}_2\text{O}$: C, 39.18; H, 6.58; N, 6.09. Found: C, 39.70; H, 6.64; N, 6.04. Anal. Calcd. for $\text{CuC}_{15}\text{H}_{28}\text{N}_2\text{Br}_4 \cdot \text{H}_2\text{O}$: C, 28.26; H, 4.74; N, 4.39. Found: C, 28.34; H, 4.76; N, 4.45.

Both crystals are unstable when exposed to moisture and became opaque upon standing in moisture under room temperature conditions. However, it is possible to store them safely by keeping them in a dry atmosphere in a desiccator or in a tightly closed vial.

Physical Measurements. Elemental analyses were carried out using a Profile HV-3 Elemental Analyzer System (Germany) at the Korean Basic Science Institute (Pusan Branch).

Magnetic susceptibility measurements were made on a powdered sample over the temperature range of 5 K to 300 K with a Quantum Design MPMS7-SQUID susceptometer at the Korean Basic Science Institute (Seoul Branch). The data were corrected for the diamagnetism of the constituent atoms with Pascal's constants.

X-ray Single Crystal Structure Determination. Crystals **1** and **2** for X-ray analysis were obtained by slow evaporation from concentrated HCl and HBr aqueous solution, respectively. A yellow crystal of **1** of approximate dimensions $0.43 \times 0.36 \times 0.30$ mm and a dark violet crystal of **2**, $0.30 \times 0.23 \times 0.20$ mm, were mounted and aligned on a CAD-4 diffractometer.¹⁸ The accurate cell parameters were refined from the setting angles of 25 reflections with $11.49^\circ < \theta < 12.75^\circ$ for **1** and 24 reflections with $11.51^\circ < \theta < 12.67^\circ$ for **2**. 2910 independent reflections for **1** in an asymmetric unit in range $-1 \leq h \leq 10$, $0 \leq k \leq 19$, $0 \leq l \leq 21$ and 3096 independent reflections for **2** in an asymmetric unit in range $-1 \leq h \leq 11$, $0 \leq k \leq 19$, $0 \leq l \leq 21$ were collected using graphite-monochromated Mo $K\alpha$ radiation and $\omega/2\theta$ scan mode.

All non-H atoms were found by the direct method and their parameters were refined successfully by full matrix least-squares. The weights used for least-squares refinement were $w^{-1} = [\sigma^2(F_o)^2 + (0.0428P)^2 + 0.5569P]$ for **1** and $w^{-1} = [\sigma^2(F_o)^2 + (0.0457P)^2]$ for **2**, where $P = (F_o^2 + 2F_c^2)/3$ is a function of intensity. All H atoms except two H atoms (H1 and H9 of **1**) were geometrically positioned and fixed. Empirical absorption corrections were applied to the intensity data for crystals **1** and **2** by using psi-scans (T_{\max} and T_{\min} are 0.6129 and 0.5409 for **1**, and 0.3429 and 0.2209 for **2**, respectively). Data collection and cell refinement: CAD4 Express.¹⁹ Data reduction: XCAD4.²⁰ Program used to solve structure and to refine structure: SHELXS97 and SHELXL97.²¹ Molecular graphics: ORTEP-3 for Windows.²² Crystallographic data for the structures reported here have been deposited with the Cambridge Crystallographic Data Centre (Deposition No. CCDC-231154 and CCDC-231155). The data can be obtained free of charge via www.ccdc.cam.ac.uk/perl/catreq/catreq.cgi (or from the CCDC, 12 Union Road, Cambridge CB2 1EZ, UK; Fax: +44-1223 336033; E-mail: deposit@ccdc.cam.ac.uk).

Table 1. Crystallographic data of **1** and **2**

	1	2
Chemical Formular	$\text{CuC}_{15}\text{H}_{30}\text{Cl}_4\text{N}_2\text{O}$	$\text{C}_{15}\text{H}_{30}\text{Br}_4\text{CuN}_2\text{O}$
FW (amu)	459.75	637.59
Crystal Description	Yellow, Block	Dark Violet, Block
Crystal Size (mm)	$0.43 \times 0.36 \times 0.3$	$0.3 \times 0.23 \times 0.2$
Crystal System	Orthorhombic	Orthorhombic
Space Group	$P2_12_12_1$	$P2_12_12_1$
T(K)	293(2)	293(2)
Radiation (MoK α) ($\lambda/\text{\AA}$)	0.71073	0.71073
<i>a</i> (\AA)	8.3080(10)	8.4769(7)
<i>b</i> (\AA)	14.6797(19)	15.166(3)
<i>c</i> (\AA)	16.4731(17)	16.679(3)
<i>V</i> (\AA^3)	2009.0(4)	2143.3(6)
Z	4	4
D_{calcd} (Mgm^{-3})	1.520	1.975
μ (mm^{-1})	1.624	8.477
F(0 0 0)	956	1244
Intensity Variation (%)	2%	3%
Independent Reflections	2910	3069
Observed Reflections	2268	1711
Final R and ωR	0.0433 and 0.0878	0.0617 and 0.0990
Threshold Expression	$I > 2\sigma(I)$	$I > 2\sigma(I)$
Parameters	224	208
$(\Delta/\sigma)_{\max}$	0.999	1.000
$\Delta\rho_{\max}$ and $\Delta\rho_{\min}$ ($\text{e}\text{\AA}^{-3}$)	0.479 and -0.285	0.625 and -0.763
Goodness of Fit	1.073	1.023
Flack Parameter	-0.04(3)	0.00(3)

Results and Discussion

Structure. The X-ray structures of crystals **1** and **2** were determined; the crystallographic data and structural refinement parameters are summarized in Table 1. Views of the molecular structures of **1** and **2** are shown in Figure 1, and the pertinent bond length and angle information for the two crystals are given in Tables 2 and 3. The structures of both **1** and **2** consist of the same basic structural units of $[\text{C}_{15}\text{H}_{28}\text{N}_2]^{2+}$, CuX_4^{2-} ($\text{X} = \text{Cl}^-$ and Br^-), and one water molecule, held together by the hydrogen bonding interactions as shown in Figure 2. There are several different types of hydrogen bonding interactions present in the crystal structures; in both crystals **1** and **2**, the doubly protonated sparteinium group form one hydrogen bond with a halogen atom of the CuX_4^{2-} unit and another hydrogen bond with an oxygen atom of a water molecule. The water molecule forms a bifurcated hydrogen bonds to two *cis*-Cl atoms of the CuCl_4^{2-} unit and another hydrogen bond with a Cl atom in **1**. However, the water molecule does not form a bifurcated hydrogen bond in **2**. Overall, the crystals **1** and **2** are stabilized into their crystal structures via the various types of hydrogen bonding interactions and the inclusion of a water molecule in **1** and **2** seems essential for the stabilization of their molecular packing structures.

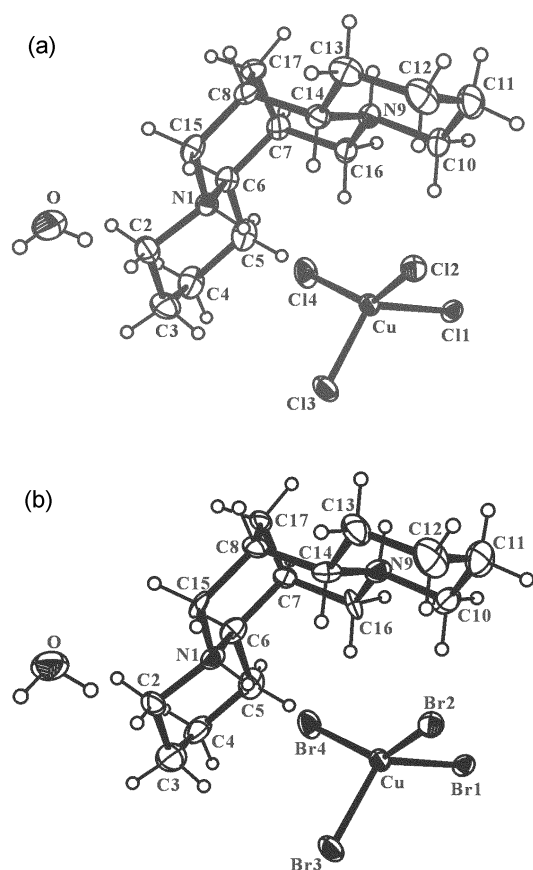


Figure 1. ORTEP diagram showing the labeling scheme in crystal **1** (a) and **2** (b).

Table 2. Selected bond distances (Å) for the complexes **1** and **2**

1			
Cu-Cl1	2.3429(13)	N1-H1	0.92(5)
Cu-Cl2	2.2169(15)	N9-C10	1.503(6)
Cu-Cl3	2.2472(15)	N9-C14	1.499(6)
Cu-Cl4	2.1998(15)	N9-C16	1.476(6)
N1-C2	1.510(6)	N9-H9	0.88(8)
N1-C6	1.517(6)	O-HO2	0.69(7)
N1-C15	1.497(6)	O-HO3	0.70(8)
2			
Cu-Br1	2.459(2)	N1-H1	0.91
Cu-Br2	2.356(2)	N9-C10	1.506(14)
Cu-Br3	2.380(2)	N9-C14	1.503(15)
Cu-Br4	2.344(2)	N9-C16	1.481(14)
N1-C2	1.509(14)	N9-H16	0.91
N1-C6	1.493(14)	O-HO2	0.863(9)
N1-C15	1.510(14)	O-HO3	0.846(9)

The conformations of four rings of doubly protonated sparteinium cations both in crystals **1** and **2** are in the form of chair-chair-boat-chair, while the conformations of free (–)-sparteine base and monoprotonated (–)-sparteinium cation are reported to be in all chair forms.²³ As described in scheme **1**, (–)-sparteine and its epimers are known to

Table 3. Selected bond angles (°) for the complexes **1** and **2**

1			
Cl1-Cu-Cl2	97.91(5)	C2-N1-H1	110(3)
Cl1-Cu-Cl3	120.20(6)	C6-N1-H1	106(3)
Cl1-Cu-Cl4	102.30(6)	C15-N1-H1	106(3)
Cl2-Cu-Cl3	100.71(6)	C10-N9-H9	109(5)
Cl2-Cu-Cl4	135.29(7)	C14-N9-H9	100(5)
Cl3-Cu-Cl4	102.70(6)	C16-N9-H9	112(5)
HO2-O-HO3	114(10)	C7-C17-C8	107.6(4)
2			
Br1-Cu-Br2	98.62(7)	C2-N1-H1	106.8
Br1-Cu-Br3	122.05(9)	C6-N1-H1	106.8
Br1-Cu-Br4	101.56(8)	C15-N1-H1	106.8
Br2-Cu-Br3	100.63(8)	C10-N9-H9	107.1
Br2-Cu-Br4	135.91(10)	C14-N9-H9	107.1
Br3-Cu-Br4	101.08(8)	C16-N9-H9	107.1
HO2-O-HO3	96.8(10)	C7-C17-C8	107.3(10)

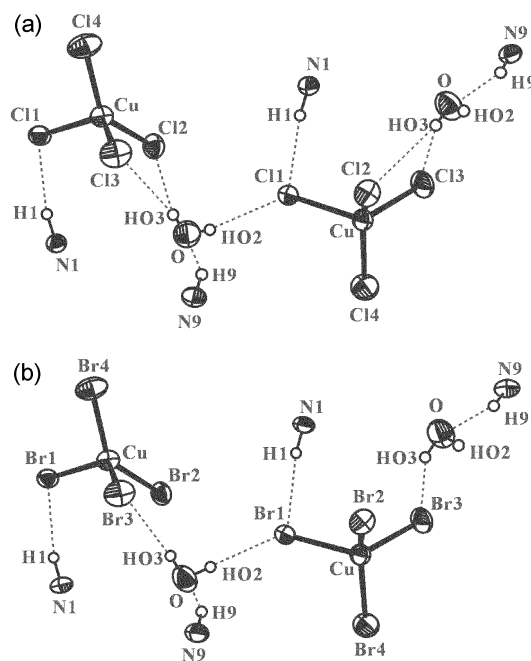
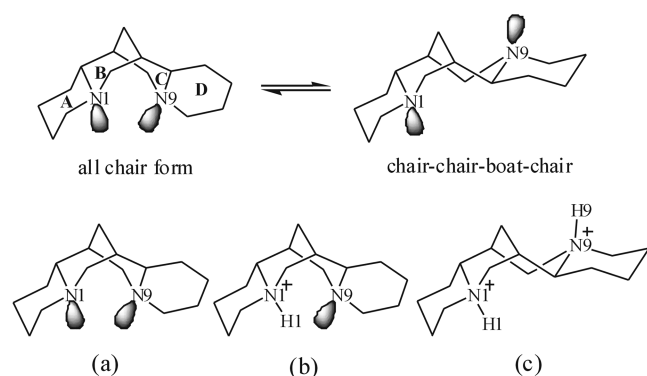


Figure 2. Illustration of a portion of the hydrogen bonding networks in the structures of **1** (a) and **2** (b).

undergo its conformational-configurational rearrangement in solution.²⁴ It is reasonable to suggest that the “chair-chair-boat chair” conformation provides much less steric repulsion between two protons, and only this conformation allow the formation of doubly protonated sparteinium cations.

As far as the geometries of $CuCl_4^{2-}$ and $CuBr_4^{2-}$ anions are concerned, the Cu-Cl distances are in the range 2.199–2.343 Å, and the Cu-Br distances are in the range 2.344–2.459 Å, both being similar to those usually found for analogous compounds. The shortest bond distance (Cu-Cl4) in **1** is 2.1998(15) Å and the shortest bond distance (Cu-Br4) in **2** is 2.344(2) Å. These results are well expected since only Cl4 and Br4 halogen atoms in CuX_4^{2-} units do not participate in



Scheme 1. Possible conformational rearrangement of (-)-sparteine base in solution, and conformations of (a) (-)-sparteine base, (b) monoprotonated (-)-sparteinium and (c) doubly protonated (-)-sparteinium in solid.

Table 4. Hydrogen bonding geometry (\AA , $^\circ$) for **1** and **2**

1				
D-H...A	D-H	H...A	D...A	\angle D-H...A
N1-H1...Cl1 ⁱ	0.92(5)	2.37(5)	3.280(4)	167(4)
N9-H9...O ⁱⁱ	0.88(8)	1.99(8)	2.795(7)	152(7)
O-HO2...Cl1 ⁱⁱⁱ	0.69(7)	2.53(7)	3.204(7)	167(9)
O-HO3...Cl2 ⁱ	0.70(8)	2.86(9)	3.407(6)	137(9)
O-HO3...Cl3 ⁱ	0.70(8)	2.73(8)	3.333(8)	146(9)
2				
D-H...A	D-H	H...A	D...A	\angle D-H...A
N1-H1...Br1 ⁱ	0.91	2.53	3.429(10)	168.2
N9-H9...O ⁱⁱ	0.91	1.96	2.806(15)	154.0
O-HO2...Br1 ⁱⁱⁱ	0.863(9)	2.5047(14)	3.368(10)	177.8(7)
O-HO3...Br2 ⁱ	0.846(9)	2.8963(16)	3.599(10)	141.6(7)
O-HO3...Br3 ⁱ	0.846(9)	2.7484(17)	3.416(10)	136.9(7)

Symmetry code: (i) $-x+1, y+1/2, -z+1/2$, (ii) $x+2, y-1/2, -z+1/2$ and (iii) $x, y+1, z$

Table 5. Dihedral angles ($^\circ$) between two X-Cu-X (X = Cl and Br) planes for CuCl_4^{2-} unit in **1** and CuBr_4^{2-} unit in **2**

Compound	Plane 1	Plane 2	Dihedral angle
1	Cl1-Cu-Cl2	Cl3-Cu-Cl4	70.79(5)
	Cl1-Cu-Cl3	Cl2-Cu-Cl4	89.12(5)
	Cl1-Cu-Cl4	Cl2-Cu-Cl3	70.07(5)
2	Br1-Cu-Br2	Br3-Cu-Br4	69.22(7)
	Br1-Cu-Br3	Br2-Cu-Br4	89.12(6)
	Br1-Cu-Br4	Br2-Cu-Br3	68.54(7)

the hydrogen bonding interactions in **1** and **2**.

The CuCl_4^{2-} and CuBr_4^{2-} anions both present a compressed tetrahedral geometry with two bond angles distinguishing their high values (120.20° and 135.29° in CuCl_4^{2-} ; 122.05° and 135.91° in CuBr_4^{2-}) from the rest (97.91 – 102.7° in CuCl_4^{2-} and 98.62 – 101.08°). The mean *trans* angle in crystals **1** and **2** are 76.7° and 75.6° , respectively, which are smaller than 90° for the perfect tetrahedron. The dihedral angles between the two X-Cu-X planes (X = Cl or Br) in

trans position are summarized in Table 5.

The interatomic distance between the two nearest copper atoms in **1** and **2** are 8.221 \AA and 8.372 \AA , respectively. The nearest non-bonded distances between the copper and halogen atom in **1** and **2**, are 5.950 \AA and 5.980 \AA respectively, too far to allow the formation of a dimeric unit with Cu-Cl-Cu or Br-Cu-Br bridges. The intermolecular distances between the two nearest halogen atoms in crystals **1** and **2** are 4.523 \AA and 4.560 \AA , respectively.

Magnetic Properties. Magnetic data for crystals **1** and **2** was collected as a function of temperature (5–300 K). As shown in Figure 3a, magnetic susceptibility data for **1** follows the Curie-Weiss law in the whole temperature range 5–300 K, yielding $\theta = -1.5 \times 10^{-4} \text{ K}$ and $C = 0.44 \text{ cm}^3 \text{ Kmol}^{-1}$, and indicating the simple paramagnetism of **1**. Magnetic susceptibility data for **2** also follows the Curie-Weiss law above 20 K, yielding $\theta = -6.1 \text{ K}$ and $C = 0.44 \text{ cm}^3 \text{ Kmol}^{-1}$. Below 20 K, however, there is a marked deviation from Curie-Weiss behavior. Figure 3b shows a plot of magnetic susceptibility vs. temperature for **2** in the low temperature region (5–60 K). The susceptibility curves exhibit a broad maximum at 6.2 K indicating a weak anti-ferromagnetic coupling. From the broad shape of the curve, and the fact that the susceptibility does not appear to tend to

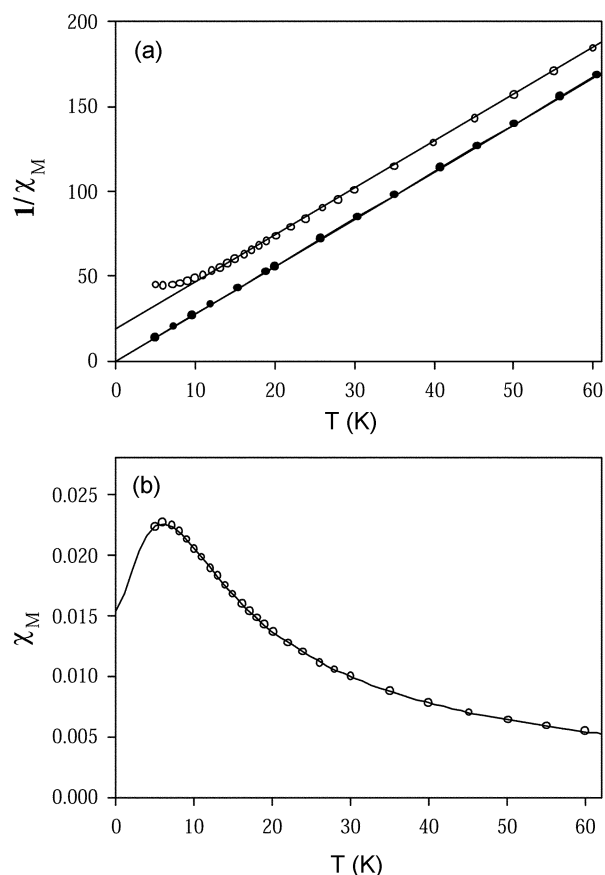


Figure 3. (a) Plots of reciprocal susceptibility vs. temperature for crystals **1** (●) and **2** (○). The solid lines are the best fits to the Curie-Weiss law. (b) Plot of magnetic susceptibility vs. temperature in the lower temperature region for crystal **2**.

zero as the temperature approaches zero, it is probable that the infinite linear chain model should be able to account for the observed susceptibility.

The magnetic data has been analyzed using the theoretical expression (the Hamiltonian being $H = -2J \sum \hat{S}_i \hat{S}_j$) proposed by Hall²⁵ for a uniform chain of local spin $S = 1/2$ (equation 1) where $A = 0.25$, $B = 0.14995$, $C = 0.30094$, $D = 1.00$, $E = 1.9862$, $F = 0.68854$, $G = 6.0626$, $\chi = |J|/kT$, and J is the exchange coupling parameter describing the magnetic interaction between any two nearest neighbor $S = 1/2$ spins.

$$\chi_M = \frac{Ng^2\beta^2}{kT} \cdot \frac{A + B\chi + C\chi^2}{D + E\chi + F\chi^2 + G\chi^3} \quad (1)$$

The above expression resulted from the numerical results of Bonner and Fisher²⁶ and has been widely used for the analysis of magnetic data. The best fit was obtained by minimizing the sum of the deviations squared times the temperature squared, i.e., $R = \sum (x_i^{calcd} - x_i^{obsd})^2 \cdot T_i^2$. The fitting results are $J = -3.24 \text{ cm}^{-1}$ and $g = 2.14$. The experimental g value of **2** at 77 K is 2.127. Several super-exchange pathways can be considered for the explanation of the observed weak anti-ferromagnetism of **2**. The interatomic distance between the two nearest copper atoms (8.372 Å) in **2** is also too long to allow the direct dipolar interaction between them. The hydrogen bonding interactions in **2** and the resulting linear chain might be considered to be a possible exchange pathway. However, if the hydrogen bonding interactions provide the exchange pathway in **2**, one might expect to observe a certain degree of anti-ferromagnetism in **1** which, in contrary, exhibits a simple paramagnetism. The Br...Br contact distance of 4.560 Å in **2** is longer by ~0.66 Å than the sum of the van der Waals radii of two bromine atoms (3.90 Å),²⁷ but is in the range of typical Br...Br contact distances (3.86-4.60 Å), usually observed in the anti-ferromagnetic tetrabromocuprate compounds.^{3,10,12} The Cl...Cl contact distance (4.523 Å) in **1** is considerably longer than the sum of van der Waals radii of two chlorine atoms (3.60 Å)²⁷ and still much longer than the longest Cl...Cl separation of 4.11 Å reported to provide a path way for magnetic exchange between monomeric $[CuCl_5]^{3-}$ anions in crystals of $[Co(NH_3)_6][CuCl_5]$.²⁸ As a result, the magnetic super exchange via the Cu-Cl...Cl-Cu contact is not likely to be observed in **1**, which actually exhibits simple paramagnetism as opposed to the anti-ferromagnetic behavior of **2**. The difference in magnetic behaviors of **1** and **2** is most probably attributable to the differences in the "halide-halide" contact distances and to the different degree of magnetic orbital overlaps in **1** and **2**.

The magnitude of the "halide-halide" contact interaction are known to depend also on the geometry of the super-exchange pathway through such parameters as the mean *trans* angle of the $CuBr_4^{2-}$ ion and the dihedral angle between the two Cu-Br...Br planes.^{11,29} In **2**, the torsion angle of the Cu-Br1...Br2-Cu contact pathway is -139.8° , and the Cu-Br1...Br2 and Br1-Br2-Cu angles are 172.9° and 116.0° , respectively. The chain is formed along the *b* axis of

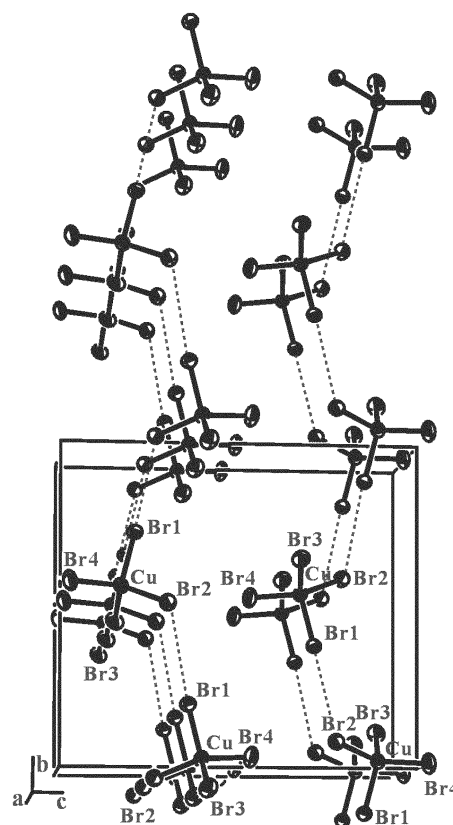


Figure 4. Crystal packing of the $CuBr_4^{2-}$ units in **2**, along with the path of exchange interaction. The Br...Br contact (denoted by dashed lines) distance is 4.560 Å.

2 (Figure 4) and the Br...Br interaction is mainly the intra-chain type. The inter-chain type of interaction can be neglected; the nearest inter-chain Br...Br distance is 4.560 Å.

From the comparative magneto-structural investigation of **1** and **2**, we suggest that the magnetic super-exchange for the weak antiferromagnetic interaction in crystal **2** occurs most probably through the Cu-Br...Br-Cu contacts denoted by dashed lines in Figure 4.

Acknowledgement. This work was supported by the Korean Research Foundation Grant (KRF-2003-002-C00130).

References

- Desjardins, S. R.; Penfield, K. W.; Cohen, S. L.; Musselman, R. L.; Solomon, E. I. *J. Am. Chem. Soc.* **1983**, *105*, 4590.
- McDonald, R. G.; Riley, M. J.; Hitchman, M. A. *Inorg. Chem.* **1988**, *27*, 894.
- Straatman, P.; Block, R.; Jansen, L. *Phys. Rev. B* **1984**, *29*, 1415.
- Halvorson, K. E.; Patterson, C.; Willett, R. D. *Acta Cryst. B* **1990**, *46*, 508.
- Llopis, M. J.; Alzuet, G.; Martin, A.; Borrás, J.; Garcia-Granda, S.; Diaz, R. *Polyhedron* **1993**, *12*, 2499.
- Weselucha-Birczynska, A.; Oleksyn, B.; Paluszkiwicz, C.; Sliwinski, J. *J. Mol. Struct.* **1999**, *511-512*, 301.
- Bontchev, P. R.; Ivanova, B. B.; Bontchev, R. P.; Mehandjiev, D. R. *Polyhedron* **2001**, *20*, 231.

8. Valdes-Martinez, J.; Alstrum-Acevedo, J. H.; Toscano, R. A.; Hernandez-Ortega, S.; Espinosa-Perez, G.; West, D. X.; Helfrich, B. *Polyhedron* **2002**, *21*, 409.
 9. Kim, Y. I.; Lee, Y. M.; Kang, S. K.; Choi, S. N. *Bull. Korean Chem. Soc.* **2002**, *23*, 1321.
 10. Snively, L. O.; Haines, D. N.; Emerson, K.; Drumheller, J. E. *Phys. Rev. B* **1982**, *26*, 5245.
 11. Long, G. S.; Wei, M.; Willett, R. D. *Inorg. Chem.* **1997**, *36*, 3102.
 12. Landee, C. P.; Turnbull, M. M.; Galeriu, C.; Giantsidis, J.; Woodward, F. M. *Phys. Rev. B* **2001**, *63*, 100402/1.
 13. Marzotto, A.; Clemente, D. A.; Benetollo, F.; Valle, G. *Polyhedron* **2001**, *20*, 171.
 14. Luque, A.; Sertucha, J.; Castillo, O.; Romàn, P. *Polyhedron* **2002**, *21*, 19.
 15. Escrivá, E.; Server-Carrió, J.; Garcia-Lozano, J.; Folgado, J.-V.; Sapina, F.; Lezama, L. *Inorg. Chim. Acta* **1998**, *279*, 58.
 16. Rubenaker, G. V.; Walpak, S.; Hutton, S. R.; Haines, D. N.; Drumheller, J. E. *J. Appl. Phys.* **1985**, *57*, 3341.
 17. Lee, Y. M.; Kim, Y. K.; Jeong, H. C.; Kim, Y. I.; Choi, S. N. *Bull. Korean Chem. Soc.* **2002**, *23*, 404.
 18. Enraf-Nonius *CAD-4 Software; version 5.0*; Delft: The Netherlands, 1989.
 19. Enraf-Nonius *CAD4 Express*; Delft: The Netherlands, 1994.
 20. Harms, K.; Wocadlo, S. *XCAD4, Program for Processing CAD-4 Diffractometer Data*; University of Marburg: Germany, 1995.
 21. Sheldrick, G. M. *SHELXL97 and SHELXS97, Program for Refinement of Crystal Structures*; University of Göttingen: Germany, 1997.
 22. Farrugia, L. J. *J. Appl. Cryst.* **1997**, *30*, 565.
 23. Lee, Y.-M.; Shim, Y.-B.; Lee, S. J.; Kang, S. K.; Choi, S.-N. *Acta Cryst. C* **2002**, *58*, o733.
 24. Boczon, W.; Koziol, B. *J. Mol. Struct.* **1997**, *403*, 171.
 25. Hall, J. W. *PhD. Dissertation*; University of North Carolina: Chapel Hill, NC, USA, 1977.
 26. Bonner, J. C.; Fisher, M. E. *Phys. Rev. A* **1964**, *135*, 640.
 27. Pauling, L. *The Nature of Chemical Bonding*, 3rd Ed.; Cornell Univ. Press: Ithaca, 1960; p 260.
 28. Straatman, P.; Block, R.; Jansen, L. *Phys. Rev. B* **1984**, *29*, 1415.
 29. Hatfield, W. E.; Jones Jr., E. R. *Inorg. Chem.* **1970**, *9*, 1502.
-